Transcriptome Response to Embolism Formation in Stems of *Populus trichocarpa* Provides Insight into Signaling and the Biology of Refilling[1][W][OA]

Francesca Secchi*, Matthew E. Gilbert, and Maciej A. Zwieniecki

Arnold Arboretum, Harvard University, Boston, Massachusetts 02131 (F.S., M.A.Z.); and Organismic and Evolutionary Biology, Harvard University, Cambridge, Massachusetts 02138 (M.E.G.)

The mechanism of embolism repair in transpiring plants is still not understood, despite significant scientific effort. The refilling process is crucial to maintaining stem transport capacity and ensuring survival for plants experiencing dynamic changes in water stress. Refilling air-filled xylem vessels requires an energy and water source that can only be provided by adjacent living parenchyma cells. Here, we report an analysis of the transcriptome response of xylem parenchyma cells after embolism formation in *Populus trichocarpa* trees. Genes encoding aquaporins, ion transporters, and carbohydrate metabolic pathways were up-regulated, and there was a significant reduction in the expression of genes responding to oxidative stress. Thus, a novel view of the plant response to embolism emerges that suggests a role for oxygen in embolized vessels as a signal triggering xylem refilling and for the activity of cation transport as having a significant role in the generation of the energy gradient necessary to heal embolized vessels. These findings redefine current hypotheses surrounding the refilling phenomenon and provide insight into the complexity of the biological response to the seemingly simple physical event of xylem embolism formation.

Embolism is caused by the formation of air bubbles in the xylem of plants, often under drought conditions (Tyree et al., 1994; Davis et al., 2002; Holbrook and Zwieniecki, 2008). The presence of embolism reduces stem capacity to transport water, and its effect can magnify leaf water stress, forcing stomatal closure and reducing leaf photosynthetic activity (Brodribb and Jordan, 2008). Under very negative xylem pressure, runaway cavitation may occur, resulting in plant death (Sperry et al., 1998). It has been demonstrated that many plant species counter embolism formation with refilling processes that can occur despite the presence of moderate tension (Tyree and Sperry, 1989; Sperry, 2003). In such instances, the process of refilling requires that embolized vessels be filled with water against existing energy gradients. Thus, refilling cannot happen spontaneously, necessitating physiological activities that would generate water flow into the empty vessel. Currently, we lack a full understanding of the biology behind this process, although several proposals and comprehensive hypotheses of how this might happen have been put forward (Salleo et al., 1996; Holbrook and Zwieniecki, 1999; Wheeler and Stroock, 2008; Zwieniecki and Holbrook, 2009).

Existing models of refilling suggest that living parenchyma cells, adjacent to the xylem vessels, are at the forefront of this process (Salleo et al., 2004). They are assumed (1) to generate an energy gradient that allows water to flow into empty vessels, (2) to supply water for the refilling, and (3) to sense embolism formation. To resolve the first task, the initial research focus has been on finding the source of the refilling energy through analysis of the carbohydrate pool in the parenchyma cells and the role of phloem in the delivery of sugars to sustain refilling. Both visualization techniques and enzymatic analysis of nonstructural carbohydrates demonstrated that starch content in *Laurus nobilis* and *Populus trichocarpa* stem parenchyma cells decreased following embolism occurrence (Salleo et al., 2009; Nardini et al., 2011; Secchi and Zwieniecki, 2011). Furthermore, the drop in starch content was associated with changes in gene expression levels of α- and β-amylases in the stems of *P. trichocarpa* (Secchi and Zwieniecki, 2011). Experiments that damaged phloem continuity resulted in decreased capacity for refilling; thus, it was concluded that phloem might be involved in supplying energy (Bucci et al., 2003; Salleo et al., 2004). The fate of sugars released from starch degradation during refilling is unknown. If sugars are transported out of the parenchyma, they might generate osmotic gradients driving water flow from the parenchyma to embolized vessels. Sugars could also be used indirectly to generate active ion efflux into the xylem apoplast via respiration.

[1] This work was supported by the National Science Foundation (grant no. IOS–0919729) and the Air Force Office of Scientific Research.

* Corresponding author; e-mail fsecchi@oeb.harvard.edu.

The author responsible for distribution of materials integral to the findings presented in this article in accordance with the policy described in the Instructions for Authors (www.plantphysiol.org) is: Francesca Secchi (fsecchi@oeb.harvard.edu).

[W] The online version of this article contains Web-only data.

[OA] Open Access articles can be viewed online without a subscription.

www.plantphysiol.org/cgi/doi/10.1104/pp.111.185124

Thus, the question regarding the role of the carbohydrate pool in refilling remains open.

The second task of the parenchyma cells requires them to supply and/or transfer water to embolized vessels. The visual evidence from cryo-scanning electron microscopy studies, magnetic resonance imaging observations, or computed tomography scans shows that vessels fill up with water during refilling (Holbrook et al., 2001; Clearwater and Goldstein, 2005) and that water droplets preferentially form on the vessel walls adjacent to parenchyma cells (Brodersen et al., 2010). However, these studies do not provide any indication of whether the water required for refilling is supplied by parenchyma cells or phloem. Indirect evidence, from analysis of aquaporin expression (plasma membrane intrinsic proteins; PIP1 and PIP2 gene subfamilies) in embolized stems, supports the notion that cell membranes play a role in water movement toward the refilling vessels. Expression levels of several PIP1 and PIP2 genes were shown to increase during the refilling process in a few species, including *P. trichocarpa* and *Juglans regia* (Sakr et al., 2003; Kaldenhoff et al., 2008; Secchi and Zwieniecki, 2010, 2011). While such changes are similar to those following the development of water stress due to drought, it is important to note that even in well-watered plants, embolism that was artificially induced through air injection resulted in significant upregulation of a subset of PIP proteins in *P. trichocarpa* (Secchi and Zwieniecki, 2011). Nonetheless, we are still missing a comprehensive picture that includes more than expression analysis of select genes.

Several lines of evidence support the hypothesis that parenchyma cells can sense embolism presence and trigger the necessary biological responses, but it is still not clear how they detect an empty vessel. It has been suggested that the initial trigger for the refilling response might come from energy released during cavitation in the form of supersonic events, and such events could be sensed via mechanosensory proteins in the cell membranes. This proposal is consistent with the observed reduction in the starch content of *L. nobilis* stems after exposure to an artificial ultrasonic source (Salleo et al., 2009). Other proposals for sensory mechanisms include effects associated with the loss of the transpiration stream in embolized vessels. In that case, it is possible that cells are not supplied with phytohormones present in the xylem sap, such as abscisic acid, or that a compound released from the cells is not transported away and is accumulated in the vicinity of parenchyma cells (Zwieniecki and Holbrook, 2009). The last proposal was recently tested on *P. trichocarpa*, with the assumption that the accumulation of Suc, or other low-molecular-mass carbohydrates, in the apoplast of embolized xylem might serve as the refilling trigger. The results demonstrated that the presence of Suc in vessels resulted in a drop of starch in stems similar to that observed after embolism induction, and there was a significant correlation in the expression changes of 20 genes between Suc and embolism treatments (Secchi and Zwieniecki, 2011).

Despite these research efforts, current knowledge about the biology of xylem refilling is limited and in need of new information to guide future research. Recent progress in genomic technologies has provided high-throughput integrated approaches to investigate global gene expression responses. Here, we report a transcriptome analysis of *P. trichocarpa* trees subjected to artificially induced embolism to provide a foundation for a better understanding of the biology behind the refilling process. Our goal was to analyze changes in the expression of genes within Gene Ontology (GO) groups across the entire transcriptome. We further compare the expression patterns of embolized stems with those of plants treated with increased Suc concentration in functional vessels to assess whether Suc and/or osmotic potential changes in the apoplast may act as a signal that triggers the refilling process.

RESULTS

Physiological Response to Treatments

Experiments were designed to avoid the generation of high tension in xylem, thus allowing for a test of expression pattern changes in response to the presence of embolism or Suc in xylem, without a confounding effect of prolonged water stress. Plants were randomly assigned to three groups: (1) generation of embolism with air injection (ET); (2) addition of Suc to growing medium (ST); and (3) control (C). Embolism formation was previously determined in plants subjected to the same treatments. Injection with pressure of −1.0 MPa to the stems increased the native embolism (measured as percentage loss of hydraulic conductivity [PLC]) from approximately 20% to more than 70%. PLC increase was not observed in control plants (Secchi and Zwieniecki, 2011). Despite the change in PLC in ET treatment or the addition of Suc in ST treatment, stem xylem tension was relatively constant for the duration of the experiment at approximately −0.6 MPa (Fig. 1). The water potential of the Suc/hydroponics solution was 1.0 MPa; thus, ST plants experienced an additional drop in the potential of apoplastic water on top of the tension in ET and C plants. In general, the stomatal conductance (g_s) of the control and ET plants remained constant during the duration of the experiment, although in a few instances ET plants displayed an initial, short-term drop in g_s (Fig. 1). However, the ST plants had a significant drop in g_s (Fig. 1). The presence of a stomatal response in ST reflects that the Suc solution applied to the growing medium reached the leaves and thus penetrated the vessels and that plants responded to lower water potential of the solution despite no change in xylem tension.

Whole Transcriptome Analysis

The experimental design included replicate microarrays performed with ET, ST, and C treatments, each

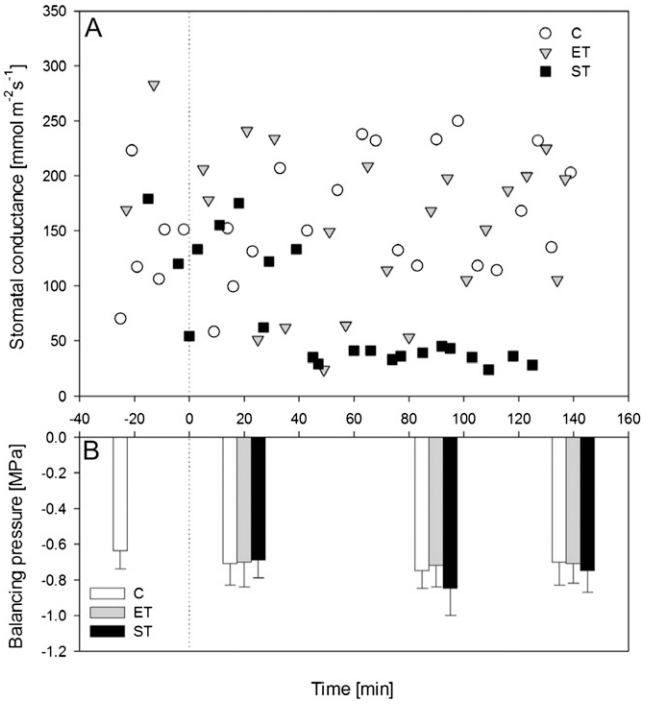

Figure 1. A, Dynamics of g_s in C, ET, and ST treatments. Time zero denotes treatment application. Each point reflects a single measurement on a randomly selected leaf from four plants included in each treatment. B, Corresponding balancing pressure of nontranspiring leaves. Bars represent averages of three measurements. No significant difference was found among treatments.

with three biological replicates of three plants (a total of 27 plants). Analyses of all microarrays using the Pearson product-moment correlation coefficient demonstrate the presence of a significant correlation within treatments, confirming that there was a treatment-specific transcriptome response (Supplemental Fig. S1). Student's t test was used to determine the significance of changes in expression between control and treatments with $\alpha < 0.1$, the threshold P value for the change to be considered significant. Of 61,410 hybridization sites analyzed, 9,430 responded significantly to ET (with 4,540 down-regulated and 4,890 up-regulated) and 8,971 responded to ST (with 4,931 down-regulated and 4,040 up-regulated; $\alpha < 0.1$). The number of hybridization sites showing a change in expression level in both treatments was significantly larger than expected from a randomization test ($P < 0.00001$; 6,141 sites; Fig. 2A).

There was a significant correlation of expression level changes between ET and ST treatments. The Pearson correlation coefficient ($r_{pearson} = 0.2501$; $P < 0.0001$) and Spearman rank correlation coefficient ($r_{spearman} = 0.3838$; $P < 0.00001$) show that ET and ST shared a significant number of genes coexpressed due to the applied treatments (Supplemental Figs. S1 and S2). More than 25% of genes with significant up- or down-regulation were coexpressed between treatments, with less than 5% showing opposite regulation (Fig. 2A). The same trend of coregulation was found using strong statistical criteria with $\alpha < 0.05$, using pooled standard deviations and with a minimum fold change of 1.2. Again, approximately 30% of genes were co-up- or co-down-regulated across both treatments, and only approximately 5% of genes showed opposite regulation between treatments (Fig. 2B). As the goal of this study was to look for general trends of transcription across the whole genome, not gene discovery, we used $\alpha < 0.1$ with no limit on fold change as the criterion for significant change in all subsequent analyses.

To validate the microarray data, we performed real-time PCR expression analyses for a subset of eight differentially expressed genes for both ET and ST treatments. We used the same RNA employed for the microarray hybridizations. All of the eight selected genes displayed expression patterns consistent with those obtained by the microarray results (Supplemental Fig. S3).

Genes Encoding Transport Proteins

ET and ST resulted in a significant number of transport protein genes (National Center for Biotechnology Information database, GO:0006810) up- or down-regulated in comparison with control plants (Fig. 3), and of these, there was a significant overlap between gene expression induced by both treatments. Bootstrap analysis suggested that the expression pattern of

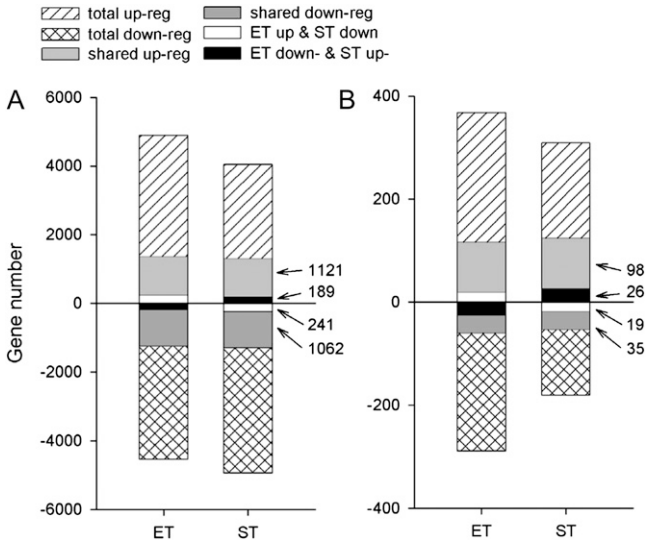

Figure 2. Number of hybridization sites (genes) that showed changes in expression level between control and treatment with threshold P value considered significant ($\alpha < 0.1$) as estimated from Student's t statistic and without a limit imposed on fold change (A) and $\alpha < 0.05$ and minimum fold change of 1.2 (B). The numbers of coexpressed and oppositely expressed genes between ET and ST treatments are also provided.

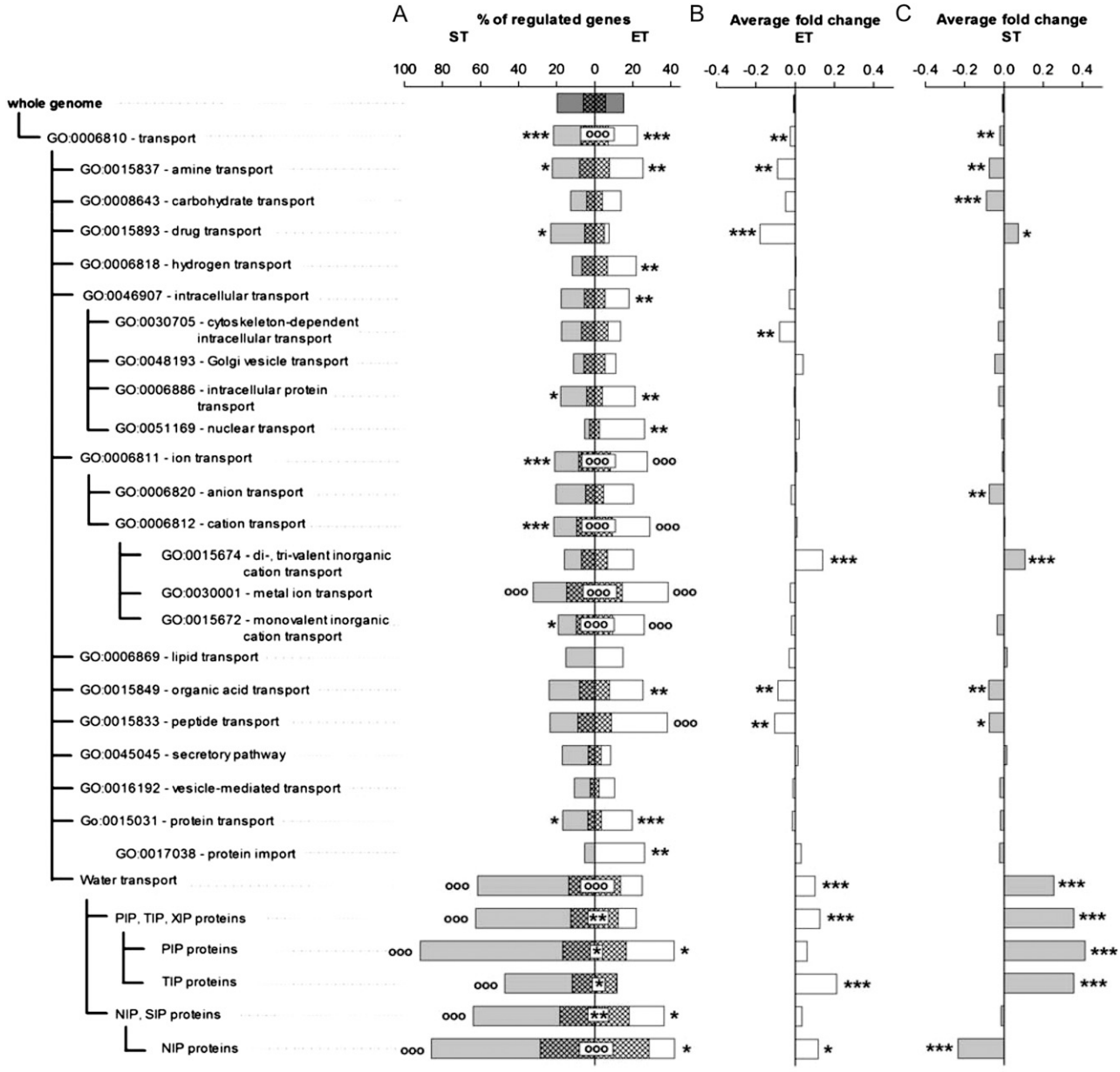

Figure 3. Transcriptomic analysis within the transport GO category (GO:0006810). A, Percentage of regulated genes for each GO category. Each gene was assumed to be regulated if its expression changed with $\alpha < 0.1$ using Student's *t* statistic. Asterisks denote significant differences between the number of genes regulated in a particular GO category and the null hypothesis that 10% of genes are regulated (randomization with 10^5 resamplings; * $P < 0.05$, ** $P < 0.01$, *** $P < 0.001$). Circles denote GO categories with the number of genes regulated significantly exceeding the predicted number based on the whole genome analysis (bootstrap with 10^5 resamplings; $\alpha < 0.05$). B and C, Average fold changes of expression for all genes in each category for ET (B) and ST (C) treatments. Asterisks denote significant differences in average expression for the GO categories tested against the whole genome (bootstrap with 10^5 resamplings).

this category of genes was not differentially expressed relative to the response of the whole genome. However, there was significant variation between specific transporter groups in the percentage of genes with significant changes in expression. In the majority of groups, gene expression was not affected by the treatments, but there was a strong effect on the percentage of genes regulated by both ET and ST in ion transporters (GO:0006811; Supplemental Fig. S4) and water channels (including all subfamilies: PIP, TIP, XIP, NIP, and SIP proteins; Supplemental Fig. S5). Specifically, ET and ST influenced the expression of metal ion transporters such that the percentage of regulated genes significantly exceeded that expected from the

genome-wide pattern (Fig. 3A; bootstrap analysis, $\alpha < 0.05$). Similarly, PIP and TIP subfamilies, encoding water channels, were strongly regulated by both treatments, and in the case of ST, the percentage of genes up-regulated significantly exceeded the genome-wide expression pattern (Fig. 3A; bootstrap analysis, $\alpha < 0.05$).

Similarly, ET and ST share a general trend of gene regulation for transport categories (Fig. 3, B and C). Water channels, with an average fold change of 0.12 in ET and 0.36 in ST, were significantly up-regulated when compared with the genome-wide response average change of −0.007 ($P < 0.0001$ for both treatments from bootstrap analysis). Detailed comparative analysis of the expression of metal ion transporters in the two treatments shows a strong correlation between ST and ET ($r_{spearman} = 0.2787$; $P < 0.00001$). This correlation was significantly different from the null hypothesis of no relationship ($P < 0.00001$, randomization test). However, it was not different from the genome-wide correlation ($P = 0.87$, bootstrap analysis; Fig. 3). The expression response of water channels was more closely correlated between treatments ($r_{spearman} = 0.6466$; $P < 0.00001$), and the correlation was significantly stronger than the genome-wide correlation ($P = 0.02$, bootstrap analysis; Fig. 3). All statistical data related to the transport GO category are reported in Supplemental Table S1.

Genes Encoding Metabolic Pathways

Analysis of the expression changes of genes related to metabolic pathways (GO:0044238) shows that the number of genes regulated by ET and ST was significantly different from the pattern observed for the whole genome ($\alpha < 0.05$, bootstrap analysis). Similarly, the Spearman correlation coefficient for metabolic pathway genes between ET and ST was significantly different from the coefficient for the entire genome ($r_{spearman} = 0.306$; $P < 0.00001$). Similar to the transport protein expression pattern, there was variation in the degree to which the different metabolic pathways responded to the treatments. However, in general, the number of affected gene categories was much larger, and the degree of regulation was also much stronger, with many metabolic pathways significantly affected by the treatments (i.e. the percentage of genes regulated in many pathways exceeded the average percentage regulation of the whole genome as tested using a bootstrap technique; Fig. 4). Average fold change of expression in GO categories showed a similar trend in both treatments, although it was greater in the ET treatment (Fig. 4).

From the perspective of understanding the plant response to embolism, it is interesting that ET influenced the regulation of genes involved in carbohydrate pathways more than the presence of Suc in the xylem. The carbohydrate pathways most influenced were monosaccharide metabolism (GO:0005996; Supplemental Fig. S6), disaccharide metabolism (GO:0005984; Supplemental Fig. S7), and carbohydrate catabolism (GO:0044275). In all three groups of genes, the percentage of genes regulated under ET was significantly higher than the average percentage in the whole genome ($\alpha < 0.05$, bootstrap analysis; Fig. 4). ET resulted in general down-regulation of genes belonging to the monosaccharide metabolism pathway (−0.22 average fold change) and strong up-regulation of disaccharide pathway genes (0.48 average fold change); both values were significantly different from the whole genome change ($P < 0.00001$, bootstrap analysis; Fig. 4). All statistical data related to GO primary metabolism are reported in Supplemental Table S2.

Genes Encoding Responses to Stress

Of the genes coding for stress responses (GO: 0006950), only genes involved in responses to oxidative stress (GO:0006979) were influenced by ET and ST ($P < 0.01$, randomization analysis). For the stress gene group, gene regulation by the ET was significantly greater than the average whole genome regulation ($P < 0.001$; Fig. 5). On average, genes from the oxidative stress-responding group were down-regulated by ET versus the whole genome (−0.0925 average fold change; $P < 0.01$, bootstrap analysis). There was also a significant correlation in response to ET and ST ($r_{spearman} = 0.4991$; $P < 0.00001$; Supplemental Fig. S8). All statistical data related to GO response to stress are reported in Supplemental Table S3.

Genes Encoding Transcription Factors

Of all 64 families of transcription factor genes (predicted from the Poplar Transcription Factor Database), we analyzed the 31 groups with nine or more genes matched to Affymetrix arrays. Of these, 13 families showed significant responses to ET and ST treatments ($P < 0.01$, randomization test), but only five families showed significant overlap in regulated genes between both treatments. Bootstrap analysis revealed that eight families were more strongly and significantly regulated in ET and ST treatments than the average regulation of the entire genome ($\alpha < 0.05$), with five families showing significant overlap (Supplemental Table S4).

Families showing especially strong responses to both treatments included AP2-EREBP, bZIP, HSF, MYB, and MYB-related. Specific regulation by ET was noticed in C2H2, GARP, HB, and WRKY families, while specific ST regulation included AS2, JUMONJI, Trihelix, and ZIM. In the case of ET, the majority of families showed down-regulation, with six families significantly down-regulated and only one significantly up-regulated (WRKY). Suc treatment showed an opposite trend, with the majority of transcription factors up-regulated, with five families significantly up-regulated ($P < 0.01$) and only one down-regulated (Trihelix).

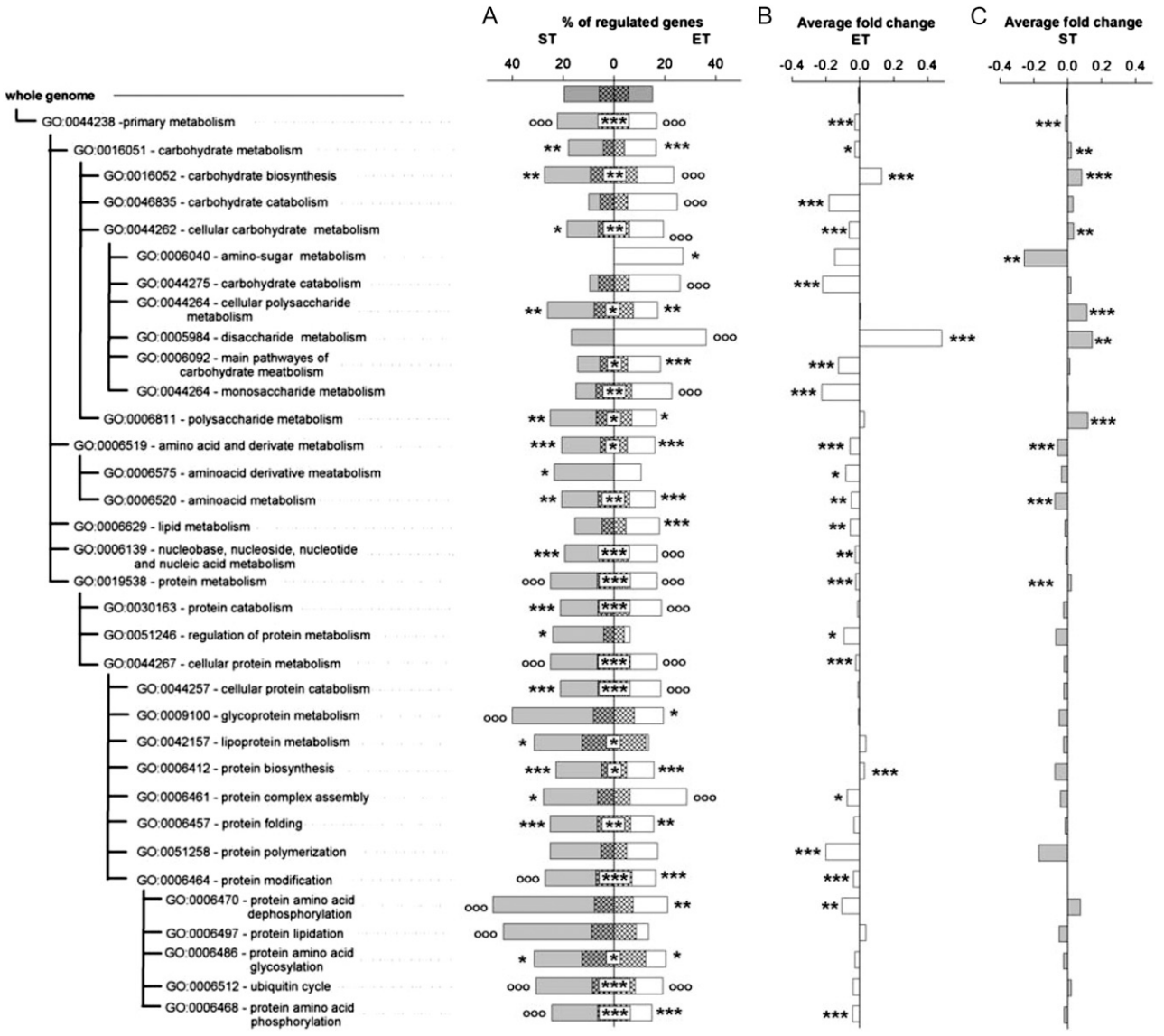

Figure 4. Transcriptome analysis within the metabolism GO category (GO:0044238). A, Percentage of genes regulated for each GO category. B and C, Average fold changes of expression for all genes in each category for ET (B) and ST (C) treatments. For symbol descriptions, see Figure 3 legend.

DISCUSSION

The refilling of embolized vessels is a combination of physical and biological processes (Zwieniecki et al., 2000; Salleo et al., 2009; Secchi and Zwieniecki, 2010, 2011). The physical part of the process has been studied using visualization techniques such as magnetic resonance imaging (Holbrook et al., 2001; Clearwater and Goldstein, 2005), microcomputed tomography scanning (Brodersen et al., 2010), experimental manipulations (Salleo et al., 2004; Zwieniecki et al., 2004), and modeling (Vesala et al., 2003). The biology of the refilling process has so far focused on studies of xylem parenchyma cells that are assumed to provide both water and energy in response to various experimental treatments (Holbrook and Zwieniecki, 1999; Zwieniecki and Holbrook, 2009; Nardini et al., 2011). Only recently have we started to get a closer look at the changes in gene expression patterns of a few groups of genes, like aquaporins (Sakr et al., 2003; Secchi and Zwieniecki, 2010, 2011). The results presented here allow, to our knowledge for the first time, a full view of the transcriptome response to the presence of embolism and provide a fundamental source of information that will lead future research in this area.

Here, the outstanding finding is that embolism formation generates a significant change in gene expression pattern in xylem parenchyma cells. The induction of embolism was not followed by any dramatic change in general plant water status, as determined by stem

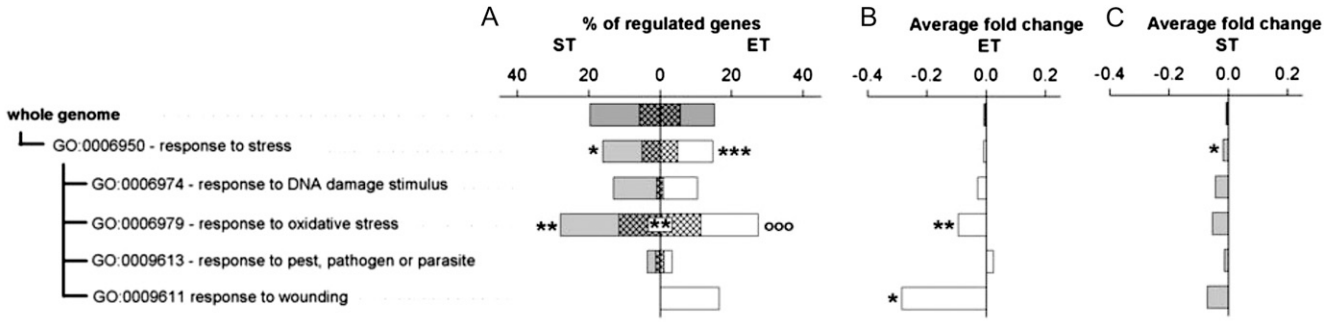

Figure 5. Transcriptome analysis within the response to stress GO category (GO:0006950). A, Percentage of genes regulated for each GO category. B and C, Average fold changes of expression for all genes in each category for ET (B) and ST (C) treatments. For symbol descriptions, see Figure 3 legend.

xylem tension and the dynamics of g_s. Thus, the observed gene regulatory response provides evidence that plants are capable of sensing embolism as a unique physical phenomenon separate from water stress. The presence of such a unique sensing mechanism was hinted at earlier based upon the behavior of starch in the stem (Salleo et al., 2009) and further developed in a theoretical analysis (Zwieniecki and Holbrook, 2009). Later, it was experimentally demonstrated in *P. trichocarpa* plants, where the expression of specific PIP water channel isoforms responded to the presence of embolism in the absence of water stress (Secchi and Zwieniecki, 2010). The signal responsible for the triggering response still remains elusive, although two competing theories exist: mechanosensing (Salleo et al., 2008) and osmoticum/Suc sensing (Zwieniecki and Holbrook, 2009), the latter being recently tested experimentally (Secchi and Zwieniecki, 2011).

Working under the assumption that changes in the osmotic (potentially Suc) properties of the embolized vessel might be the origin of the triggering signal, we included here an analysis of the transcriptome response to the infiltration of xylem with Suc. This allowed us to compare the response of xylem parenchyma to the formation of embolism with the response to osmotic stress. There was a significant, positive correlation between the transcriptome expression levels of the embolism and Suc treatments ($r_{\text{spearman}} = 0.38$; $P < 0.000001$). This positive correlation suggests that the plant response to embolism and osmoticum (or Suc) presence in xylem sap shares a significant part of the same signaling pathway. This does not conclusively support the idea that the response to embolism is triggered by the lack of water flow leading to a buildup of Suc in vessel walls, as was suggested previously (Zwieniecki and Holbrook, 2009; Secchi and Zwieniecki, 2011). In the view of our data here, an alternative signaling pathway is hypothesized. A significant down-regulation of genes responding to oxidative stress in ET suggests that embolism led to a reduction in the abundance of reactive oxygen species (ROS). This drop might be associated with changes in oxygen concentration through altered diffusion of oxygen in functional (water-filled) versus nonfunctional (embolized) vessels, leading to a reduction of hypoxia stress in parenchyma cells surrounding newly embolized vessels and a drop in ROS concentration (Fukao and Bailey-Serres, 2004).

The observed responses were not equal across GO categories, with some being disproportionately up-regulated. These included water channels and metal ion transporters. Both transport groups are known to be involved in responses to water-related stress (Vandeleur et al., 2009), although their role in refilling is not well understood. Aquaporins were indicated to play an important role in plant response to embolism and refilling (Sakr et al., 2003; Secchi and Zwieniecki, 2010, 2011), but the role of metal ion transporters in the process has not been considered. It is worthwhile to note that embolism significantly reduced the expression of genes related to carbohydrate transport. This down-regulation may suggest that the balance of uptake and leakage of sugars between cell and apoplast was shifted toward leakage, promoting the buildup of osmoticum in the refilling vessel. Interestingly, the embolism, but not sugar, treatment resulted in very strong regulation of the carbohydrate metabolic pathways in xylem parenchyma cells. In particular, embolism resulted in down-regulation of the monosaccharide metabolic pathway and strong up-regulation of the disaccharide metabolic pathway that includes starch metabolism. This result supports earlier reports that show a reduction in starch content and an increase in Suc level in parenchyma cells in response to embolism (Salleo et al., 2009; Secchi and Zwieniecki, 2011). However, in view of the limited information on the fate of Suc released during starch hydrolysis, we cannot conclude if it is used for respiration or transported out of the cell, and its role in refilling remains to be elucidated.

CONCLUSION

The analysis of the transcriptome response to embolism presented here provides a set of information that allows us to formulate a next-generation concept

of the cellular biology responsible for refilling (Fig. 6). It is evident that embolism is being sensed by the living cells surrounding the xylem and that it triggers transcription level responses for many genes. The origin of the signal might be related to osmoticum/Suc buildup in the apoplast compartment, as suggested before (Secchi and Zwieniecki, 2011); this hypothesis is supported by significant overlap of the genetic response found in this study. However, our findings may also suggest a simpler scenario, in which the presence of air in the embolized vessels triggers the initial response directly via a reduction of hypoxic stress and a reduction in ROS formation (Fig. 6).

Regardless of the origin of the signal, it results in significant expression changes of genes involved in carbohydrate metabolism. This included up-regulation of the disaccharide metabolism gene group, which contains genes involved in starch degradation, and down-regulation of genes from the monosaccharide metabolism category. Such a pattern of carbohydrate metabolism would promote the release of Suc from starch that can be used as a source of energy needed to run the refilling process either as supporting respiratory activity or as an osmoticum. The observed drop in the oxidative stress gene activity suggests that air in the embolized vessel diffuses into the parenchyma cells and most likely provides an additional boost of respiration in cells responsible for refilling. Taken together, the activity of the transcriptome described above suggests that parenchyma cells up-regulate energy production after embolism formation. This energy might be used to support ion transport (significant up-regulation of ion transporter genes) and possibly result in a change in the carbohydrate flux across the membrane (down-regulation of carbohydrate transporters). It is important to note that the use of

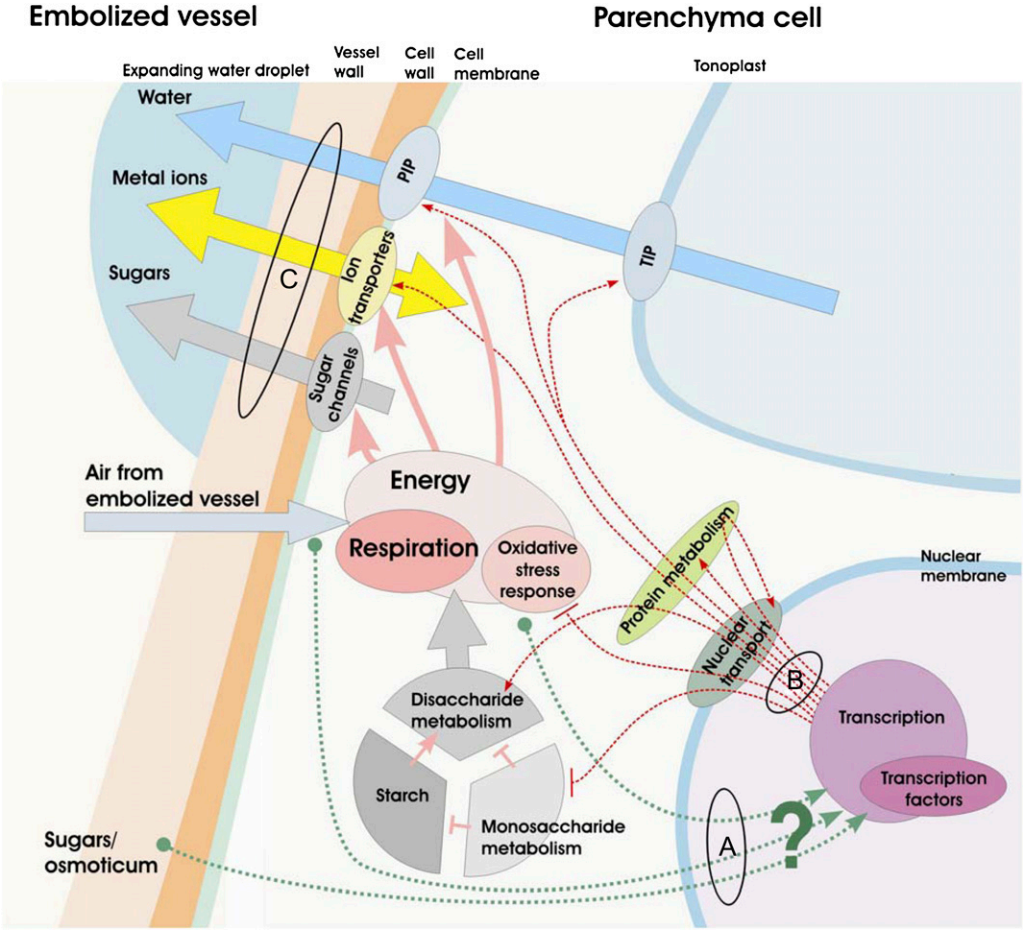

Figure 6. Schematic illustration of the proposed biological response of parenchyma cells to embolism. A, Green dashed lines denote potential signal origins (air in embolized vessels, respiratory activity, apoplastic osmoticum) that can trigger the transcriptome response or, in the case of oxygen availability, directly influence respiration and reduce oxidative stress levels. B, Red dashed lines denote major changes in transcription, as observed in this study, including transport and metabolic categories, nuclear transport, and protein metabolism. C, Arrows represent major fluxes that can be influenced by observed changes in the expression levels, including sugar, ion, and water transport pathways. Biological activity associated with the carbohydrate pool suggests the up-regulation of disaccharide metabolism and starch digestion. For more details, see "Conclusion."

carbohydrates as osmoticum for refilling would require a change in direction, from inward to outward transport activity, that could only be achieved with changes in sugar concentration and proton balance across the membrane (Geiger, 2011). The homeostasis that promotes the efflux of sugars out of cells will also require the activity of metal ion transporters to balance the "refilling" electrochemical potential. The buildup of osmoticum outside of the cell triggers an efflux of water that is additionally facilitated by strong up-regulation of water channels from the PIP and TIP subfamilies (Fig. 6).

MATERIALS AND METHODS

Plant Material and Growth Conditions

Populus trichocarpa cuttings were rooted in aerated hydroponics containers (6.5 L) filled with modified Hoagland solution [pH 6.50–7.00; 795 mM KNO_3, 603 mM $CaNO_3$, 270 mM $MgSO_4$ and 190 mM KH_2PO_4; micronutrients: 40.5 mM Fe(III)-EDTA, 20 mM H_3BO_4, 2 mM $MnSO_4$, 0.085 mM $ZnSO_4$, 0.15 mM $CuSO_4$ and 0.25 mM Na_2MoO_4] and located in a controlled-growth chamber (24°C/20°C day/night, 12 h/12 h light/dark, 70% humidity, with 500 μmol m^{-2} s^{-1} photosynthetically active radiation). After 2 to 3 weeks, the plants were transferred to 42-L boxes (12 plants per box) and allowed to grow for an additional 4 months, during which time the nutrient solution was replaced weekly.

Experimental Design and Treatments

Twenty-seven *P. trichocarpa* plants of homogeneous size were divided in three groups (each group composed of nine plants): subjected to ET, ST, and C treatment. Embolism was artificially induced through air injection into the stems of the ET plants, as described by Secchi and Zwieniecki (2010). In brief, a hole was drilled into the stem using 1.0-mm drill bit, and a small-diameter tube (0.98 mm; polyether ether ketone) was sealed into the hole using a custom-built compression fitting system that allowed for direct pressurization of the xylem. An air pressure of approximately 1 MPa was applied to the stems for 60 s, after which time the pressure was released and the tube was removed. Woody stems were collected 90 min following the injection on sections located approximately 10 cm above the hole. The ST plants were exposed to osmotic stress by adding 1 MPa of Suc (137 g L^{-1}) to the modified Hoagland solution. Prior to, and during, treatment, the Hoagland mixture was aerated, as we previously determined that lack of preaeration leads to a sudden loss of turgor. To ensure the uptake of sugar, approximately 50% of the root tips were shaved from the root system using razor blades prior to immersion in the modified solution. Wood samples were collected after 90 min of exposure to Suc. Control plants were treated exactly as treated plants, including shaved roots, a hole drilled, and chamber placement, although no pressure was applied. Wood samples were collected at the same time as treated samples.

In order to prevent contamination of the wood sample by bark or phloem, the bark was peeled and the xylem was scraped with a scalpel. The samples were immediately frozen in liquid nitrogen and kept at −80°C until molecular analyses were performed.

Stem Xylem Tension and Gas Exchange

To follow the physiological response to the treatments, another group of plants were treated in the same manner as described above, with four replicates per control or treatment. Stem xylem tension was measured for each plant using equilibrated nontranspiring (bagged) leaves. Mature leaves were covered with aluminum foil and placed in a humidified plastic bag for 15 min prior to excision and measurement. After excision, leaves were allowed to equilibrate for more than 10 min before balancing pressure was measured using a Scholander-type pressure chamber (Soil Moisture Equipment).

g_s was measured for each plant with a portable gas-exchange system (CIRAS-2; PP Systems). Leaves were measured once g_s was stable after 2 to 4 min and under the following conditions: 390 μmol mol^{-1} CO_2, 500 μmol m^{-2} s^{-1} photosynthetically active radiation, 25°C leaf temperature, and 200 μmol s^{-1} flow. Both physiological measurements were conducted before starting the treatments and were monitored throughout the experiments (180 min).

RNA Extraction and Quality Examination

Wood samples from three plants were pooled. Three biological replicates per treatment were analyzed (i.e. a total of nine plants were included in each treatment). Frozen stems were ground to a fine powder in liquid nitrogen, and total RNA was extracted from 500 mg of frozen powder according to the protocol of Chang et al. (1993). Total RNA yield and purity were determined spectrophotometrically (NanoDrop ND-1000; Thermo Scientific) at A_{260} and A_{280}. RNA integrity was assessed on an Agilent 2100 Bioanalyzer and showed no evidence of degradation.

Microarray Design, Normalization, and Data Analysis

The GeneChip Poplar Genome Array (Affymetrix; http://www.affymetrix.com/support/technical/datasheets/poplar_datasheet.pdf) was used to examine transcriptional differences of plants subjected to ET, ST, and C treatments. For each treatment, three biological replicates were analyzed. Synthesis of one-cycle cDNA and biotin-labeled complementary RNA, fragmenting of complementary RNA, hybridization to the Poplar Genome Array, washing, staining, and scanning was performed as stated by Affymetrix (GeneChips Expression Analysis Technical Manual) at the Faculty of Arts and Sciences Center for Systems Biology at Harvard University.

Gene chip results were analyzed using robust multiarray averaging, and Pearson correlation was used to determine initial correlation between signal levels and between chips. For each gene, we calculated average expression within control and embolized treatments and determined Student's t statistic to assess differences between treatments. Using a threshold P value of 0.1 ($\alpha < 0.1$), we determined the number of genes that changed expression for each GO group. To determine whether the number of regulated genes versus the size of the gene group was significantly different from the null hypothesis (that only $\alpha \times N$ genes were regulated, where α was the assumed Student's t statistic threshold and N was the number of genes within the GO group), we used a randomization procedure with 10^5 resamples. To test whether a particular group of genes was different from the ratio of genes regulated at the whole genome level, we used bootstrap analysis with 10^5 resamples for each test. To test whether average fold change within each group was different from the change of the whole genome, we used bootstrap analysis with 10^5 resamples for each test.

Biological Interpretation

The Joint Genome Institute (JGI) gene identifier numbers of genes involved in biological processes (GO:0008150) and specifically in primary metabolism (GO:0005975), transport (GO:0006810), and response to stimulus (GO:0050896) were downloaded from the *Populus* Genome Release 1.1 (Tuskan et al., 2006). The Genome Portal includes a tool for browsing through the GO database and finding genes related to GO terms. The JGI gene model identifiers of all transcription factors were downloaded from the Database of Poplar Transcription Factors (Zhu et al., 2007). The database contains 2,576 known and predicted transcription factors of *P. trichocarpa* distributed in 64 families. All of these identifiers were matched with the JGI gene identifier numbers corresponding with the Affymetrix probe, as the annotation for each Affymetrix probe set identifier consists of corresponding public identifiers, JGI poplar gene models, and predicted Arabidopsis (*Arabidopsis thaliana*) homologs and functional annotation.

Real-Time PCR

For real-time PCR, primer pairs were designed for ubiquitin as a reference gene and for eight transcripts that in microarray analysis showed significant expression changes. Primer design was performed with the Primer 3 program (Rozen and Skaletsky, 2000), and the sequences are listed in Supplemental Table S5. Total RNA was isolated according to the protocol of Chang et al. (1993), and contaminant genomic DNA was removed from the samples by digestion with RNase-free DNase I (Fermentas), following the manufacturer's instructions. cDNA was synthesized using SuperScript II Reverse Transcriptase (Invitrogen) according to the supplier's instructions using oligo$(dT)_{12–18}$

(Fermentas) as a primer. Gene transcript abundance was quantified with SYBR Green JumpStart TaqReadyMix (Sigma) on an Mx3000PTM PCR system (Stratagene). Thermocycler conditions for all real-time analyses were 95°C for 5 min, followed by 40 cycles of 95°C for 30 s, 59°C for 1 min, and 72°C for 30 s. Data were analyzed using Mx3000PTM Real-Time PCR system software (Stratagene), and the values were normalized to transcript levels of the ubiquitin gene. Real-time PCR was carried out using three biological replicates per treatment. Three technical replicates were performed for each of the three biological replicates.

All microarray data have been deposited in the National Center for Biotechnology Information Gene Expression Omnibus database with accession number GSE32322.

Supplemental Data

The following materials are available in the online version of this article.

Supplemental Figure S1. Pearson product-moment correlation matrix for gene expression for the C, ET, and ST treatments.

Supplemental Figure S2. Positive correlation of gene expression level (as log fold changes) between ET and ST.

Supplemental Figure S3. Correlation of real-time PCR expression data and microarray signal ratios.

Supplemental Figure S4. Comparative analysis of gene coexpression between ET and ST for metal ion transporters.

Supplemental Figure S5. Comparative analysis of gene coexpression between ET and ST for aquaporins.

Supplemental Figure S6. Comparative analysis of gene coexpression between ET and ST for monosaccharide metabolism.

Supplemental Figure S7. Comparative analysis of gene coexpression between ET and ST for disaccharide metabolism.

Supplemental Figure S8. Comparative analysis of gene coexpression between ET and ST for genes responding to oxidative stress.

Supplemental Table S1. Number of genes significantly regulated ($\alpha < 0.1$; i.e. with a Student's t statistic of $P < 0.1$), statistics, and average fold change for GO groups related to transport for ET, ST, and genes coregulated (shared response) between treatments.

Supplemental Table S2. Number of genes significantly regulated ($\alpha < 0.1$; i.e. with a Student's t statistic of $P < 0.1$), statistics, and average fold change for GO groups related to primary metabolism for ET, ST, and genes coregulated (shared response) between treatments.

Supplemental Table S3. Number of genes significantly regulated ($\alpha < 0.1$; i.e. with a Student's t statistic of $P < 0.1$), statistics, and average fold change for GO groups related to stress response for ET, ST, and genes coregulated (shared response) between treatments.

Supplemental Table S4. Number of genes significantly regulated ($\alpha < 0.1$; i.e. with a Student's t statistic of $P < 0.1$), statistics, and average fold change for GO groups related to transcription factors for ET, ST, and genes coregulated (shared response) between treatments.

Supplemental Table S5. Gene identifiers and sequences of primers used for quantitative real-time PCR.

Received August 8, 2011; accepted September 26, 2011; published September 27, 2011.

LITERATURE CITED

Brodersen CR, McElrone AJ, Choat B, Matthews MA, Shackel KA (2010) The dynamics of embolism repair in xylem: in vivo visualizations using high-resolution computed tomography. Plant Physiol **154:** 1088–1095

Brodribb TJ, Jordan GJ (2008) Internal coordination between hydraulics and stomatal control in leaves. Plant Cell Environ **31:** 1557–1564

Bucci SJ, Scholz FG, Goldstein G, Meinzer FC, Da L, Sternberg SL (2003) Dynamic changes in hydraulic conductivity in petioles of two savanna tree species: factors and mechanisms contributing to the refilling of embolized vessels. Plant Cell Environ **26:** 1633–1645

Chang S, Puryear J, Cairney J (1993) A simple and efficient method for isolating RNA from pine tree. Plant Mol Biol Rep **11:** 113–116

Clearwater M, Goldstein G (2005) Embolism repair and long distance transport. *In* NM Holbrook, MA Zwieniecki, eds, Vascular Transport in Plants. Elsevier, New York, pp 201–220

Davis SD, Ewers FW, Sperry JS, Portwood KA, Crocker MC, Adams GC (2002) Shoot dieback during prolonged drought in Ceanothus (Rhamnaceae) chaparral of California: a possible case of hydraulic failure. Am J Bot **89:** 820–828

Fukao T, Bailey-Serres J (2004) Plant responses to hypoxia: is survival a balancing act? Trends Plant Sci **9:** 449–456

Geiger D (2011) Plant sucrose transporters from a biophysical point of view. Mol Plant **4:** 395–406

Holbrook NM, Ahrens ET, Burns MJ, Zwieniecki MA (2001) In vivo observation of cavitation and embolism repair using magnetic resonance imaging. Plant Physiol **126:** 27–31

Holbrook NM, Zwieniecki MA (1999) Embolism repair and xylem tension: do we need a miracle? Plant Physiol **120:** 7–10

Holbrook NM, Zwieniecki MA (2008) Transporting water to the tops of trees. Phys Today **61:** 76–77

Kaldenhoff R, Ribas-Carbo M, Sans JF, Lovisolo C, Heckwolf M, Uehlein N (2008) Aquaporins and plant water balance. Plant Cell Environ **31:** 658–666

Nardini A, Lo Gullo MA, Salleo S (2011) Refilling embolized xylem conduits: is it a matter of phloem unloading? Plant Sci **180:** 604–611

Rozen S, Skaletsky HJ (2000) Primer3 on the WWW for general users and for biologist programmers. *In* S Krawetz, S Misener, eds, Bioinformatics Methods and Protocols: Methods in Molecular Biology. Humana Press, Totowa, NJ, pp 365–386

Sakr S, Alves G, Morillon RL, Maurel K, Decourteix M, Guilliot A, Fleurat-Lessard P, Julien JL, Chrispeels MJ (2003) Plasma membrane aquaporins are involved in winter embolism recovery in walnut tree. Plant Physiol **133:** 630–641

Salleo S, Lo Gullo MA, De Paoli D, Zippo M (1996) Xylem recovery from cavitation-induced embolism in young plants of *Laurus nobilis*: a possible mechanism. New Phytol **132:** 47–56

Salleo S, Lo Gullo MA, Trifilò P, Nardini A (2004) New evidence for a role of vessel-associated cells and phloem in the rapid xylem refilling of cavitated stems of Laurus nobilis L. Plant Cell Environ **27:** 1065–1076

Salleo S, Trifilò P, Esposito S, Nardini A, Lo Gullo MA (2009) Starch-to-sugar conversion in wood parenchyma of field-growing *Laurus nobilis* plants: a component of the signal pathway for embolism repair? Funct Plant Biol **36:** 815–825

Salleo S, Trifilò P, Lo Gullo MA (2008) Vessel wall vibrations: trigger for embolism repair? Funct Plant Biol **35:** 289–297

Secchi F, Zwieniecki MA (2010) Patterns of PIP gene expression in *Populus trichocarpa* during recovery from xylem embolism suggest a major role for the PIP1 aquaporin subfamily as moderators of refilling process. Plant Cell Environ **33:** 1285–1297

Secchi F, Zwieniecki MA (2011) Sensing embolism in xylem vessels: the role of sucrose as a trigger for refilling. Plant Cell Environ **34:** 514–524

Sperry JS (2003) Evolution of water transport and xylem structure. Int J Plant Sci **164:** S115–S127

Sperry JS, Adler FR, Campbell GS, Comstock JP (1998) Limitation of plant water use by rhizosphere and xylem conductance: results from a model. Plant Cell Environ **21:** 347–359

Tuskan GA, Difazio S, Jansson S, Bohlmann J, Grigoriev I, Hellsten U, Putnam N, Ralph S, Rombauts S, Salamov A, et al (2006) The genome of black cottonwood, Populus trichocarpa (Torr. & Gray). Science **313:** 1596–1604

Tyree MT, Kolb KJ, Rood SB, Patiño S (1994) Vulnerability to drought-induced cavitation of riparian cottonwoods in Alberta: a possible factor in the decline of the ecosystem? Tree Physiol **14:** 455–466

Tyree MT, Sperry JS (1989) Vulnerability of xylem to cavitation and embolism. Annu Rev Plant Physiol Plant Mol Biol **40:** 19–38

Vandeleur RK, Mayo G, Shelden MC, Gilliham M, Kaiser BN, Tyerman SD (2009) The role of plasma membrane intrinsic protein aquaporins in water transport through roots: diurnal and drought stress responses reveal different strategies between isohydric and anisohydric cultivars of grapevine. Plant Physiol **149:** 445–460

Vesala T, Hölttä T, Perämäki M, Nikinmaa E (2003) Refilling of a

hydraulically isolated embolized xylem vessel: model calculations. Ann Bot (Lond) **91:** 419–428

Wheeler TD, Stroock AD (2008) The transpiration of water at negative pressures in a synthetic tree. Nature **455:** 208–212

Zhu QH, Guo AY, Gao G, Zhong YF, Xu M, Huang MR, Luo JC (2007) DPTF: a database of poplar transcription factors. Bioinformatics **23:** 1307–1308

Zwieniecki MA, Holbrook NM (2009) Confronting Maxwell's demon: biophysics of xylem embolism repair. Trends Plant Sci **14:** 530–534

Zwieniecki MA, Hutyra L, Thompson MV, Holbrook NM (2000) Dynamic changes in petiole specific conductivity in red maple (*Acer rubrum* L.), tulip tree (*Liriodendron tulipifera* L.) and northern fox grape (*Vitis labrusca* L.). Plant Cell Environ **23:** 407–414

Zwieniecki MA, Melcher PJ, Feild TS, Holbrook NM (2004) A potential role for xylem-phloem interactions in the hydraulic architecture of trees: effects of phloem girdling on xylem hydraulic conductance. Tree Physiol **24:** 911–917